frontiers | Frontiers in Marine Science

TYPE Original Research
PUBLISHED 15 September 2022
DOI 10.3389/fmars.2022.999902

OPEN ACCESS

EDITED BY
Ricardo Serrão Santos,
University of the Azores, Portugal

REVIEWED BY
Abdel Galil Hewaidy,
Al-Azhar University, Egypt
Gabriela J. Arreguín-Rodríguez,
Universidad Autónoma de Baja California, Mexico

*CORRESPONDENCE
Katarzyna Melaniuk
Katarzyna.Melaniuk@uit.no

SPECIALTY SECTION
This article was submitted to Deep-Sea Environments and Ecology, a section of the journal Frontiers in Marine Science

RECEIVED 21 July 2022
ACCEPTED 25 August 2022
PUBLISHED 15 September 2022

CITATION
Melaniuk K, Sztybor K, Treude T, Sommer S, Zajączkowski M and Rasmussen TL (2022) Response of benthic foraminifera to environmental successions of cold seeps from Vestnesa Ridge, Svalbard: Implications for interpretations of paleo-seepage environments. *Front. Mar. Sci.* 9:999902. doi: 10.3389/fmars.2022.999902

Response of benthic foraminifera to environmental successions of cold seeps from Vestnesa Ridge, Svalbard: Implications for interpretations of paleo-seepage environments

Katarzyna Melaniuk[1]*, Kamila Sztybor[2], Tina Treude[3,4], Stefan Sommer[5], Marek Zajączkowski[6] and Tine L. Rasmussen[1]

[1]Centre of Arctic Gas Hydrate, Environment and Climate (CAGE), Department of Geosciences, UiT The Arctic University of Norway, Tromsø, Norway, [2]Fram Centre, Akvaplan-niva AS, Tromsø, Norway, [3]Department of Earth, Planetary, and Space Sciences, University of California Los Angeles, Los Angeles, CA, United States, [4]Department of Atmospheric and Oceanic Sciences, University of California Los Angeles, Los Angeles, CA, United States, [5]GEOMAR Helmholtz Centre for Ocean Research Kiel, Kiel, Germany, [6]Department of Paleoceanography, Institute of Oceanology of Polish Academy of Sciences, Sopot, Poland

This paper presents the results of a study on the response of living benthic foraminifera to progressing environmental successions in a cold-seep ecosystem. Sediment samples were collected from Vestnesa Ridge (79°N, Fram Strait) at ~1200 m water depth. The distribution of live (Rose Bengal-stained) foraminifera were analyzed in the upper sediment layers in relation to pore water biogeochemical data together with the distribution of sulfur-bacterial mats and *Siboglinidae* tubeworms. At methane cold seeps, the process of environmental succession is strongly connected to the duration and strength of methane seepage and the intensity of methane-related biological processes, e.g, aerobic and anaerobic oxidation of methane (MOx and AOM, respectively). The results show that the distribution patterns of benthic foraminifera change according to the progressing environmental succession. The benthic foraminifera seemed to thrive in sediments with a moderate activity of seepage, dominated by MOx, i.e, at an early stage of seepage or when seepage decreases at a late stage of the succession. Species composition of the foraminiferal fauna under these conditions was similar to the control sites (outside of pockmarks with no seepage); the dominant species being *Melonis barleeanus* and *Cassidulina neoteretis*. In sediments with strong seepage and high AOM activity, the hostile environmental conditions due to the presence of toxic sulfide caused a reduction in the foraminiferal population, and samples were almost barren of foraminifera. In environments of moderate methane seepage, the presence of chemosynthetic *Siboglinidae* tube worms potentially support communities of the epibenthic species *Cibicidoides*

wuellerstorfi. Despite the very different environmental conditions, the foraminiferal assemblages were very similar (or nearly absent). Therefore, the foraminiferal faunas cannot be used as exclusive indicators of past strength of methane seepage in palaeoceanographic interpretations.

KEYWORDS

Arctic, gas hydrate (clathrate), methane (CH4), benthic ecology, protista

Introduction

Benthic foraminifera are unicellular organisms, commonly occurring in a variety of marine environments. Information about the distribution and abundance of foraminiferal species carry a valuable record of past oceanic conditions, thus they are commonly used as tools in paleoclimatic and –oceanographic reconstructions (Murray, 2006; Gooday and Jorissen, 2012). In recent years, cold-seep benthic foraminifera have gained increased attention due to their potential to record changes in past degrees of methane seepage (Torres et al., 2003; Millo et al., 2005; Bernhard et al., 2010; Martin et al., 2010; Consolaro et al., 2015; Schneider et al., 2017; Sztybor and Rasmussen, 2017). There is a link between the release of methane from geological reservoirs and climate change, e.g, during the Quaternary and the Paleocene periods (Wefer et al., 1994; Dickens et al., 1997; Smith et al., 2001). A large amount of natural gas is stored in Arctic marine sediments in the form of gas hydrates or free gas. It is important to understand the fate of methane in marine sediments to understand the potential impact of ongoing methane release on Arctic ecosystems. Methane seepage from subseafloor reservoirs is manifested by the presence of cold seep ecosystems, i.e, methane-dependent, chemosynthetic faunas at the seabed. This type of ecosystem provides a good analogue for past methane-rich environments and offers an opportunity to investigate possible effects of methane seepage on benthic foraminiferal communities. Although knowledge of the ecology and distribution patterns of cold-seep-associated benthic foraminiferal species remain one key to improve the interpretation of past records, the ecology and distribution patterns of living foraminiferal species in relation to different types of seep environments are still poorly studied.

It is commonly accepted that the distribution of benthic foraminifera is mainly determined by environmental factors, such as temperature, oxygen, food availability, and CO_2 (e.g. Corliss et al., 1986; Jorissen et al., 1995; Thomas et al., 1995; Rasmussen and Thomsen, 2017). Due to the ephemeral nature of cold seeps, the above-mentioned environmental factors change over time, and so does the microhabitats in which the foraminifera live. Natural processes of changes in the faunal structure of an ecological community over time can result from the combined effects of changing environmental factors and biological interactions including among others commensalism and competition, and is referred to as environmental successions; Dayton and Hessler, 1972; Tanner et al., 1994; Chapman and Underwood, 1994). At cold seeps, the environmental successions are strongly connected to varying strengths of seepage of hydrocarbon fluids and methane-related biological processes such as aerobic and anaerobic oxidation of methane (MOx and AOM, respectively), which shape the biochemistry of the sediment. Seep community successions as modeled by Bergquist et al. (2003) and Bowden et al. (2013) suggests a general succession pattern beginning with a localized flux of methane-rich fluids which promotes growth of MOx bacterial communities at the sediment surface (Stage 1 of succession). Prolonged methane seepage causes expansion of sulfur-bacterial mats and increase in AOM activity (Stage 2). Moderate supply of sulfide between the patches of sulfur-bacterial mats can become inhabited by Vesicomyid clam populations (Stage 3). If seepage continue, colonization by *Siboglinidae* tubeworms starts. Over time, formation of authigenic carbonate rocks and pavements modifies methane flow and limit the extent of sulfide-rich sediments. As a result, Vesicomyid populations reduces in favor of the chemosynthetic *Bathymodiolus* mussels, which opposite to clams require hard substrates (Stage 4). As seepage declines, cold-water corals can colonize the authigenic carbonate rocks and eventually form large, long-lasting coral reefs in post-seepage conditions (Stage 5; Bergquist et al., 2003).

In this paper, we present the results of a study of the distribution patterns of living (Rose Bengal-stained) benthic foraminifera in the surface and near-surface sediments from a cold-seep ecosystem at Vestnesa Ridge together with the downcore distribution of pore water biogeochemical data.

Materials and methods

Study area

Vestnesa Ridge is a deep-sea ridge (>1000 m), located in the Fram Strait, west of Svalbard in the Arctic Ocean (79°N, 5–7°E;

Figure 1). Vestnesa developed under the effect of contour currents (Eiken and Hinz, 1993; Hustoft et al., 2009) and it is estimated that periodic gas seepage has occurred since 2.7 Ma from the start of the Quaternary coinciding with glacial intensification at the western Svalbard margin (Plaza-Faverola et al., 2015). On the crest of Vestnesa Ridge a series of pockmarks occur (i.e, shallow seabed depressions where methane-rich fluids seep from the seabed), among which the two most active are informally referred to as 'Lomvi' and 'Lunde' (Bünz et al., 2012; Plaza-Faverola et al., 2015). In these pockmarks, TowCam video observations have revealed the presence of cold-seep related structures such as bacterial mats, macro- and megafaunas and methane-derived authigenic carbonate outcrops (Åström et al., 2016; Sztybor and Rasmussen, 2017; Åström et al., 2018; Melaniuk, 2021).

Sediment sampling

Sediment samples for this study were collected during the POS419 expedition of RV *Poseidon* in August 2011, the CAGE 15-2 cruise in May 2015 (Melaniuk, 2021), and during the CAGE 18-3 cruise both with RV *Helmer Hanssen* to Vestnesa Ridge (Figure 1; Table 1). The two most active pockmarks were targeted. The sampling on POS419 and CAGE 15-2 cruises were done using a TV-guided multicorer to visually localize active methane seep sites within the pockmarks to select sampling spots. Porewater data for multicores MUC 10, MUC 11, and MUC 12 has been previously published (Melaniuk et al., 2022), and foraminiferal fauna data for multicores MC 893A and MC 886 in Melaniuk (2021). For this study we have added multicore MUC 8 (POS419) for additional analyses of porewater and foraminiferal faunas (Figure 1). All foraminiferal samples from POS419 (MUC 8, 10, 11, and -12, and the samples from the CAGE 18-3 cruise are new for this study.

After recovery of the multicorer, selected cores were processed on board. Cores designated for benthic foraminiferal analyses were sampled in 1-cm thick slices. For this study, the top 1-cm thick slice of sediment was used for foraminiferal analyses. The sediment from POS419 was transferred into plastic containers and stained with a Rose Bengal-ethanol solution following the FOBIMO protocol (2 g L^{-1}; Schönfeld et al., 2012). For details of sampling during the CAGE 15-2 cruise see Melaniuk (2021). During the CAGE 18-3 cruise, sediment samples were collected using a box corer (50 x 50 x 50 cm). The top 1 cm of the sediment was collected using a spatula and placed in plastic container with Rose Bengal-ethanol solution (2 g L^{-1}; Schönfeld et al., 2007). For one station, a subcore was taken for geochemical analyses.

Rose Bengal was used in this study to make our results comparable with most other studies. All samples were kept onboard in a dark, cool (+4°C) room until further processing (for details see Melaniuk, 2021; Melaniuk et al., 2022).

Three cores collected from each station of the POS419 cruise were designated for the analyses of 1) sediment pore water chemistry, 2) sediment methane concentration, and 3) rates of microbial methane oxidation and sulfate reduction. All sediment sampling procedures were conducted at +4°C inside a cooled laboratory (for details see Melaniuk et al., 2022).

Foraminiferal analyses

Sediment samples from POS419 were sieved through a 100-µm sieve. The >100-µm residue of each sample was kept wet in distilled water and further examined under reflected-light

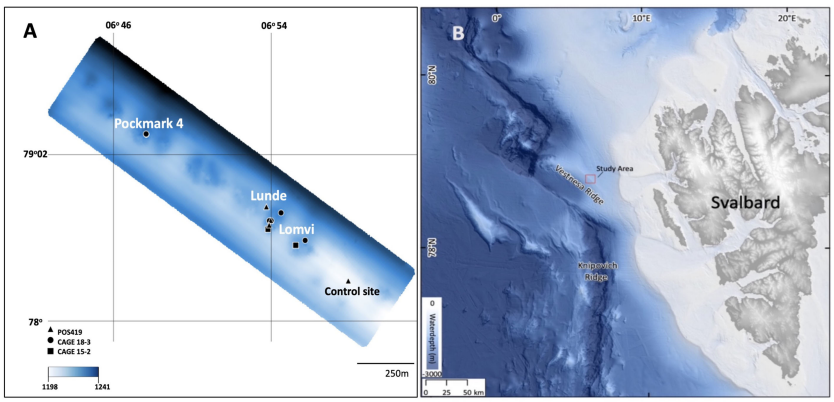

FIGURE 1
(A) Detail of Vestnesa Ridge (modified from Bünz et al., 2012). Triangles indicate POS419 multicorer locations, dots indicate CAGE 18-3 box core locations, and squares CAGE 15-2 multicorer locations **(B)** Svalbard margin in the Eastern Fram Strait (bathymetry from (Jakobsson et al., 2020).

TABLE 1 Sampling locations, coordinates, water depth, date of sampling, environmental characteristics and analyses performed at sampling sites.

Cruise ID	MUC ID	Location	Coordinates	Depth (m)	Date	Analyses
POS419	MUC 10	'Lunde' pockmark	79°.00.466′ 06°54.279′	1241	25.08.2011	Foraminiferal faunas sulfide, SO_4^{2-}, total alkalinity, methane, AOM, sulfate reduction
POS419	MUC 8	'Lunde' pockmark	79°00.600 06°54,094′	1204	25.08.2011	Foraminiferal faunas sulfide, SO_4^{2-}, total alkalinity, methane, AOM, sulfate reduction
POS419	MUC 12	'Lunde' pockmark	79°00.417′ 06°54.131′	1235	29.08.2011	Foraminiferal faunas sulfide, SO_4^{2-}, total alkalinity, methane, AOM, sulfate reduction
POS419	MUC 11	Control site	79°59.774′ 06°58.064′	1191	28.08. 2011	Foraminiferal faunas
CAGE 15-2	MC 893*	'Lomvi' pockmark	79°00.187′ 06°55.440′	1200	20.05.2015	Foraminiferal faunas
CAGE 15-2	MC 886*	'Lunde' pockmark	79°00.381′ 06°54.040′	1200	20.05.2015	Foraminiferal faunas
CAGE 18-3	BC 1081	'Lunde' pockmark	79°00.459′ 06°54.268′	1206	15.07.2018	Foraminiferal faunas
CAGE 18-3	BC 1082	'Lunde' pockmark	79°00.459′ 06°54.166′	1206	15.07.2018	Foraminiferal faunas
CAGE 18-3 subcore	BC 1082	'Lunde' pockmark	79°00.459′ 06°54.166′	1206	15.07.2018	SO_4^{2-}
CAGE 18-3	BC 1088	'Lunde' pockmark	79°01.463′ 06°48.023′	1212	16.07.2018	Foraminiferal faunas
CAGE 18-3	BC 1090	Lunde' pockmark	79°00.524′ 06°53.857′	1205	16.07.2018	Foraminiferal faunas
CAGE 18-3	BC 1098	Pockmark 4	79°02.199′ 0°43.655′	1217	16.07.2018	Foraminiferal faunas
CAGE 18-3	BC 1099	'Lunde' pockmark	79°01.465′ 06°48.016′	1212	16.07.2018	Foraminiferal faunas
CAGE 18-3	BC 1101	'Lomvi' pockmark	79°00.235′ 06°55.908′	1208	16.07.2018	Foraminiferal faunas

*, data from Melaniuk (2021).

microscopy. Rose Bengal-stained foraminifera representing both live and recently dead (but still containing cytoplasm) individuals were wet picked, counted and identified. Individuals that stained dark magenta and were fully filled with cytoplasm were considered 'living' foraminifera (i.e, live + recently dead individuals). Empty, unstained tests were omitted and not counted in this study. The numbers of living (Rose Bengal stained) foraminifera were compared using Student's *t*-test ($\alpha = 0.05$). The Shannon index S(H) of diversity of species, Evenness index which refers to how close in numbers each species in a sample is, and a Chao1 index for estimating the number of species in a sample (Table S1) were calculated for each sample. Rose Bengal-stained sediment samples collected during CAGE 15-2 and CAGE 18-3 were sieved through a 63-µm sieve (see details in Melaniuk, 2021).

Porewater analyses

Porewater data MUC 10 and 12 have been previously published (Melaniuk et al., 2022; see Supplementary Information). For this study, we have added the pore water data for MUC 8 following the same methods as in Melaniuk et al. (2022).

Porewater from MUC 8 was extracted at +4°C using a low-pressure squeezer (argon at 1–5 bar) onboard the vessel and right after sampling. While squeezing, porewater was filtered through 0.2 µm cellulose acetate nuclepore filters and collected in argon-flushed recipient vessels. The collected porewater samples were analyzed onboard for their content of dissolved total sulfides (in the following referred to as "sulfide") (Cline, 1969). 50 µl of zinc acetate solution was added to a 1-ml sample of pore water. Subsequently, 10 µl of N,N-dimethyl-1,4-phenylenediamine-dihydrochloride color reagent solution and 10 µl of the $FeCl_3$ catalyst were added and mixed. After 1 hour of reaction time, the absorbance was measured at 670 nm. Total alkalinity (TA) was determined by direct titration of 1 mL pore water with 0.02 M HCl using a mixture of methyl red and methylene blue as an indicator. Bubbling the titration vessel with argon gas was performed to strip CO_2 and hydrogen sulfide. The analyses were calibrated using the IAPSO seawater standard, with a precision and detection limit of 0.05 mmol L^{-1}. Porewater samples for sulfate (SO_4^{2-}) analyses were stored in 2-ml glass vials at +4°C and analyzed onshore. Sulfate was determined by

ion chromatography (Metrohm, IC Compact 761). Analytical precision based on repeated analysis of IAPSO standards (dilution series) was <1%.

Methane measurements

Methane concentrations in MUC 8 were determined in 1 cm intervals down to a depth of 6 cm followed by 2 cm intervals down to 12 cm, 3 cm intervals down to 18 cm and 5 cm intervals deeper than 18 cm (Sommer et al., 2009). From each level, a 2 mL sub-sample was transferred into a septum-stoppered glass vial (21.8 ml) containing 6 ml of saturated solution of NaCl and 1.5 g of NaCl in excess. The volume of headspace was 13.76 ml. Within 24 h, the methane concentration in the headspace was determined using a Shimadzu GC 14A gas chromatograph fitted with a flame ionization detector and a 4 m × 1/8-inch Poraplot Q (mesh 50/80) packed column. Prior to the measurements the samples were equilibrated for 2 h on a shaking table. The precision to reproduce a methane standard of 9.98 ppm was 2%.

Microbial methane oxidation rates

On board, radioactive methane ($^{14}CH_4$ dissolved in water, injection volume 15 µl, activity ~5 kBq, specific activity 2.28 GBq mmol^{-1}) was injected into three replicate mini cores at 1-cm intervals according to the whole-core injection method (Jørgensen, 1978). The mini cores were incubated at *in-situ* temperature for ~24 h in the dark. To stop bacterial activity, the sediment cores were sectioned into 1-cm intervals and transferred into 50-ml crimp glass vials filled with 25 ml of sodium hydroxide (2.5% w/w). After crimp-sealing, glass vials were shaken thoroughly to equilibrate the pore-water methane between the aqueous and gaseous phase. Control samples were first terminated before addition of tracer. In the home laboratory, methane oxidation rates and methane concentrations in the sample vials were determined according to Treude et al. (2020).

Microbial sulfate reduction rates

Sampling, injection, and incubation procedures were the same as for the methane oxidation samples. The injected radiotracer here was carrier-free $^{35}SO_4^{2-}$ (dissolved in water, injection volume 6 µl, activity 200 kBq, specific activity 37 TBq mmol^{-1}). To stop bacterial activity after incubation, sediment cores were sectioned into 1-cm intervals and transferred into 50 ml plastic centrifuge vials filled with 20 ml zinc acetate (20% w/w) and frozen. Control sediment was first terminated before addition of tracer. In the home laboratory, sulfate reduction rates were determined according to the cold-chromium distillation method (Kallmeyer et al., 2004).

Results

Habitat characteristics

Based on visual and geochemical characteristics, the investigated samples have been assigned to individual stages of the environmental succession of the seep sites (Table 2).

TABLE 2 Sites characteristics.

Environmental succession of seeps	Core ID	Sites characteristic
Stage 1	MC 893A*,	Patchy distributed sulfur-bacterial mats, sediment not smelly,
	BC 1090	No *Siboglinidae* tube worms
	BC 1101	Low seepage
Stage 2	MC 886*	Densely covered with sulfur-bacterial mats
	MC 893B	Top sediment black, anoxic, presence hydrogen sulfide (H_2S)
	MUC 12 A, B**	Strong seepage
Stages 3	BC 1088	Thin oxidized layer < 1 cm above black, smelly mud, H_2S present
	BC 1098	1 cm oxidized layer above grey mud, smelly,
	BC 1099	2-cm thick oxidized layer above grey mud; smelly sediment, few *Siboglinidae* tube worms, strong to moderate seepage
Stage 4	BC 1082	Dead bivalves – Rhagothyas/Thyasira; *Siboglinidae* tube worms
	BC 1081	Densely covered with *Siboglinidae* tube worms
	MUC 10A, C**	Oxidized layer present, moderate seepage
	MUC 8	
Stage 5	Has not been observed at Vestnesa Ridge	

*Melaniuk, 2021; **Melaniuk et al., 2022.

Sediments of the *Siboglinidae* field from MUC 8 showed only modest signs of methane seepage activity. Sulfate showed only a small but steady decline from seawater concentration (28.8 mM) to 27.5 mM at 0 to 30 cm depth (Figure 2M). The methane concentration profile showed two different slopes: a modest increase in concentration from the surface reaching 15 µM at 16.5 cm, and a steeper increase below 16.5 cm reaching 88 µM at depth 30 cm (Figure 2M). The change in slope could possibly marks the lower end of sediment irrigation by *Siboglinidae* tubes. Sulfide was generally low (<10 µM) with sporadic peaks at the surface, at 9 cm, and at 16.5 cm (Figure 2R). No AOM data are available for MUC 8 and only one sulfate reduction replicate was obtained (Figure 2E, I). Sulfate reduction was low (< 2 nmol cm^{-3} $d^{->3}$) throughout the core with no activity at the sediment-water interface and a distinct peak (max 1.6 nmol cm^{-3} d^{-3}) at 6.5 cm and a second, smaller peak (0.56 nmol cm^{-3} d^{-3}) at 14.5 cm. The fact that methane concentration steeply increased below 16.5 cm suggests that the second peak in sulfate reduction was related to methane-dependent AOM, while the shallower peak might be correlated to organoclastic sulfate reduction. The sulfate concentration in sediment in BC 1082 is close to the seawater concentration (28,8 mM; Figure 2P). No AOM data, methane, sulfate reduction rates, total alkalinity and sulfide are available for BC 1082 (Figure 2D, H, L, U).

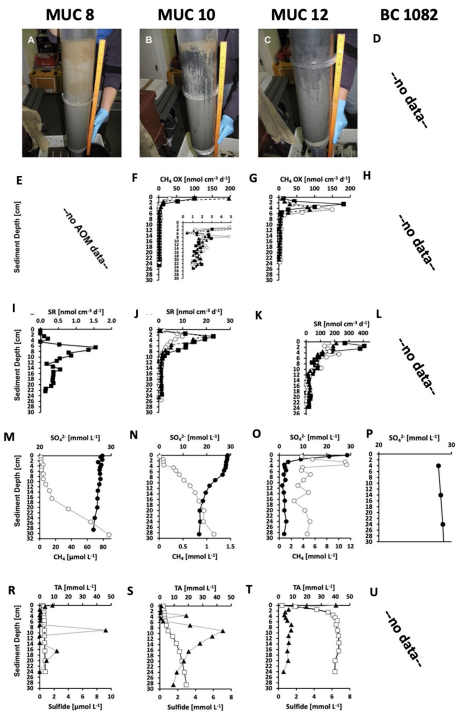

FIGURE 2
(A, B, C) Selected sediment core photos and biogeochemical parameters of MUC 8 (Stage 4, left panels, note the visible tubes at the surface), MUC 10 (Stage 4, middle panels, note the visible tubes at the surface), and MUC 12 (Stage 2, right panels, note the foamy sediment consistency caused by degassing). Note the different units for methane and sulfide in MUC 8. Data from MUC 10 and 12 were previously published in Melaniuk et al. (2022). P) Concentration of sulfate in sediment from BC 1082. Data courtesy T. Laier, Geological Survey of Denmark and Greenland (GEUS), Copenhagen, Denmark. **(E, F, G)** Methane oxidation rates (CH_4 OX, symbols represent three replicates). **(I, J, K, L)** Sulfate reduction rates (SR, symbols represent three replicates). **(M, N, O, P)** Concentrations of pore-water sulfate (SO_4^{2-}, solid circles) and sediment methane (CH_4, open circles). Note the different x-axes for methane. **(R, S, T, U)** Concentrations of pore-water total alkalinity (TA, open squares), and sulfide (solid triangles).

Foraminiferal faunas

The results show variations in the density of foraminifera according to the succession of seep environments. The early Stage 1 of low methane release showed density of foraminifera from 7 to 25 individuals per 10 cm^3 (Figure 3). In Stage 2 of strong seepage, the density decreased to 3 individuals per 10 cm^3 (Table S1). The number of foraminifera increased in the Stage 3 of moderate seepage from 24 to 32 individuals per 10 cm^3. At Stage 4, also of moderate seepage, the number of foraminifera ranged from 25 to 99 individuals per 10 cm^3 of sediment. (Figure 3; Table S1). Student's t-test (p = 0.09; α = 0.05) showed no statistical difference between the number of foraminifera at Stage 4 of the environmental succession and the control site of no seepage, and no significant differences between Stage 3 and Stage 4 (p = 0.12; α = 0.05) (both stages of moderate seepage). Further, student's t-test showed statistical differences between number of foraminifera in Stages 1, 2, 3, and the control site of no seepage (Figure 3).

Rose bengal-stained agglutinated foraminifera contributed between 10 to 39% of the total foraminiferal fauna at Stage 1, between 0 to 69% at Stage 2, between 26 to 29% at Stage 3, and between 22 to 65% at Stage 4, and 54–55% of total foraminiferal assemblages at the control site (Figure 4). Student's t-test showed no statistical differences between number of agglutinated foraminifera at Stage 1, Stage 2, Stage 3, and control site (p = 0.00, p = 0.00; p = 0.01; α = 0.05, respectively; Figure 4). There are no statistical differences between number of agglutinated foraminifera at Stage 1, Stage 3 (p = 0.05; α = 0.05) and between Stage 1 and Stage 4 (p = 0.05, α = 0.05; Figure 4). There were further significant differences in the number of agglutinated foraminifera at Stage 3 and Stage 4 (p = 0.16; α = 0.05), Stage 4 and the control site of no seepage (p = 0.94; α = 0.05).

The Shannon index S(H) ranged from 1,65 to 2,42 at Stage 1, from 0,81 to 1,76 at Stage 2, from 2,11 to 2,52 at Stage 3, from 1,96 to 2,17 at Stage 4, and from 1,98 to 2,03 at the control site. The Evenness index ranged from 0,52 to 0,87 at Stage 1, from 0,78 to 1,13 at Stage 2, from 0,51 to 0,65 at Stage 3, from 0,51 to 0,63 at Stage 4, and from 0,56 to 0,63 at the control site.

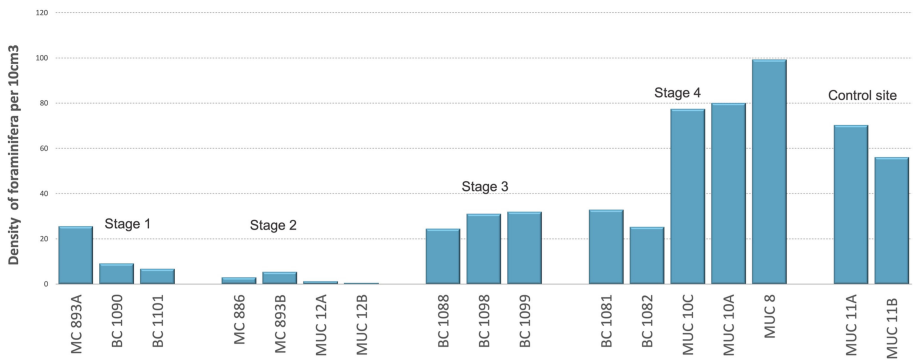

FIGURE 3
Number of Rose Bengal-stained foraminifera (calcareous and agglutinated) for each Stage (S) of environmental succession, per 10 cm^3 of the sediment. Student's t-tests: S1: S2 p = 0.01; S1: S3 p = 0.00; S1: 4 p = 0.03; S1: control site p = 0.00; S2: S3 p = 0.00; S2: S4 p = 0.00; S2: controls p = 0.00; S3: S4 p = 0.12; S3: control p = 0.01; S4: control site p = 0.09.

In samples corresponding to Stage 1 of the environmental succession the most common species was *Melonis barleeanus* and *Cassidulina neoteretis*. *Melonis barleeanus* constituted to 12–53% of the total number of calcareous foraminifera, and *C. neoteretis* ranged from 18 to 38 (Figure 5). Stage 2 was dominated by *M. barleeanus*, which constituted between 50–76% of the calcareous species. At Stage 3 the most abundant species was *C. neoteretis* (13–35%), and *M. barleeanus* (12–51%) (Figure 5). In the surface sediment in core BC 1088 *Bolivina pseudopunctata* constituted up to 31% of the calcareous species. At Stage 4, *C. neoteretis* represented between 32 and 52% of the benthic foraminiferal fauna and *M. barleeanus* 5 to 35% (Figure 5). In samples from MUC 10A *Cibicides wuellerstorfi* reached 19% (Figure 5).

Discussion

Distribution patterns of living foraminiferal faunas

Samples collected at Vestnesa Ridge represent four potential stages of environmental successions of the seep ecosystems according to the model suggested by Bergquist et al. (2003) (Figure 6). The process depends on the intensity and duration of methane seepage and is manifested by changes in the distribution patterns of the benthic foraminiferal faunas. For example, appearance of filamentous sulfur-bacterial mats (e.g, *Beggiatoa* sp.) characterizes the Stages 1 and 2 of the succession, and symbiont-bearing animals (e.g, *Siboglinidae*, bivalves)

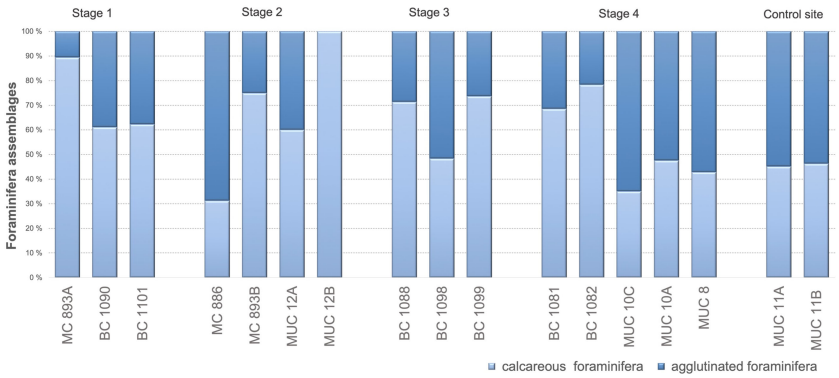

FIGURE 4
Percentage ratio between calcareous and agglutinated foraminifera for each Stage (S) of environmental succession; direct counting. S1: S2 p = 0.04; S1: S3 p = 0. 05; S1: S4 p = 0.05; S1: control site p = 0.00; S2: S3 p = 0.02; S2: S4 p = 0.06; S2: control site p = 0.00; S3: S4 p = 0.16; S3: control p = 0.01; S4: control site p = 0.94.

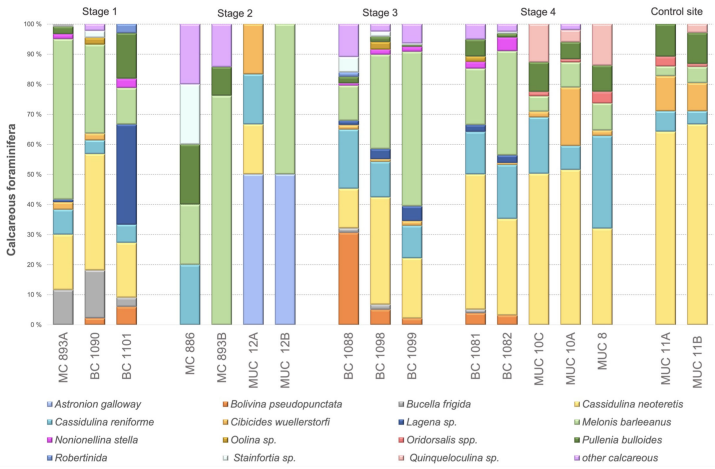

FIGURE 5
Percentage of Rose Bengal-stained calcareous foraminiferal species (direct count).

characterize Stage 4, when seepage is slowing down, and sulfide conditions are stable (Bergquist et al., 2003; Levin, 2005). We observed that the distribution patterns and ecological successions of the benthic foraminiferal faunas are closely related to the properties and environmental succession of the different microhabitats and thus the species composition of the foraminiferal faunas changes according to the progressing environmental succession. The sampling location of MC 893, BC 1090, and BC 1101 represent Stage 1 of the environmental succession. The TowCam imaging survey during the sampling campaign of the CAGE 15-2 cruise showed that the sediment surface close to MC 893 was covered by patchily distributed white and grey filamentous sulfur-bacteria in areas where methane was leaking from the sediment (Yao et al., 2019; Dessandier et al., 2019; Melaniuk, 2021). The methanotrophic bacterial community at site MC 893 was not well developed yet, implying that the seepage by advective methane transport *via* mini-fractures at this location started relatively recently (Yao et al., 2019). These authors suggested that the seepage at site MC 983 most likely started a year prior to the sampling in 2015 (Yao et al., 2019). At Stage 1, Rose Bengal-stained foraminifera are present (Melaniuk, 2021), with the Shannon index between 1,65 to 2,42. Parallel to other foraminiferal faunas from cold-seeps, the fauna at Stage 1 is dominated by species adapted to low oxygen and high organic content; here *M. barleeanus* and *C. neoteretis* (Rathburn et al., 2000; Bernhard et al., 2001; Hill et al.,

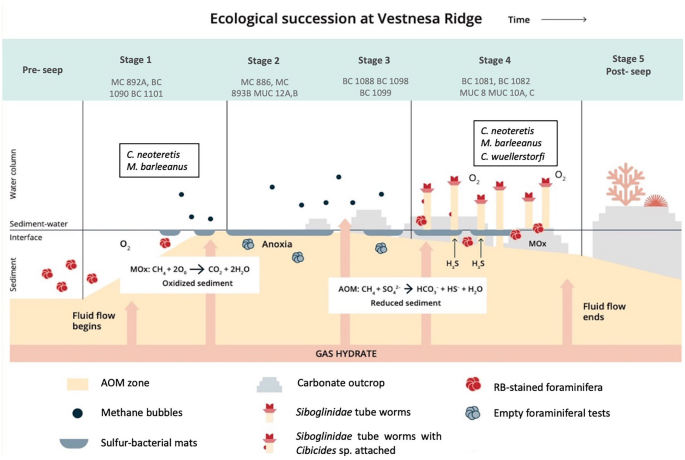

FIGURE 6
The proposed course of environmental and ecological successions at Vestnesa Ridge. Stage 5 has not (yet) been observed at Vestnesa.

2003; Herguera et al., 2014; Etiope et al., 2014) (Figure 5). These two species are common on the mid-slope in the Nordic Seas (Sejrup et al., 1989; Mackensen et al., 1985; Wollenburg and Mackensen, 1998), and are usually present within non-seep marine environments, and previously reported at both seep- and non-seep sites at Vestnesa Ridge (Sztybor and Rasmussen, 2017; Dessandier et al., 2019; Melaniuk, 2021). *Melonis barleeanus* is an intermediate to deep infaunal species (i.e, a species which live within the sediment) associated with high-nutrient conditions and resistant to environmental stress due to organic matter degradation (Wollenburg and Mackensen, 1998; Alve et al., 2016). Methanotrophic-like bacteria have previously been found in close proximity to the apertural region of living *M. barleeanus* suggesting that methane-related bacteria can be a part of the diet of *M. barleeanus* (Bernhard and Panieri, 2018). *Cassidulina neoteretis* is a shallow infaunal species living in the sediment surface layer and presently one of the most common species at Arctic cold seeps such as at Vestnesa Ridge (Dessandier et al., 2019; Melaniuk, 2021), Storfjordrenna pingo sites (Melaniuk, 2021), and Ha°Ckon Mosby Mud Volcano (Wollenburg and Mackensen, 2009).

Prolonged methane seepage causes oversaturation of methane in the sediment and lead to the development of a microbial AOM community. The environmental succession moves to Stage 2, represented by MUC 12A, B, MC 893B, and MC 886 in this study. The sediments become dark grey to black in color, release a strong smell of sulfide, are anoxic and reduced below the sediment surface (Figure 2C, T). The sediment of MUC 12 was densely covered by sulfur bacterial mats and dominated by AOM and sulfate reduction developing high concentrations of H_2S just below the sediment surface (Figure 2G, K, O; Melaniuk et al., 2022). The geochemistry of site MC 886 was described earlier by Yao et al. (2019). The authors estimated that methane seepage at site MC 886 started earlier compared to the seepage at site MC 893 and that the methane transport was characterized by diffusion (Yao et al., 2019). We suggest that the distribution patterns of the benthic foraminifera at Stage 2 in the environmental succession in MC 886 mainly are controlled by the presence of sulfide released from the AOM consortium of archaea and sulfate reducers. Sulfide is considered highly toxic for aerobic marine organisms as it inhibits production of ATP (aadenosine triphosphate) by irreversibly binding to cytochrome c oxidase (Somero et al., 1989). Compared to Stage 1, food availability seems to play only a secondary role for the foraminiferal community. As a result of adverse environmental conditions, samples from MUC 12 were almost completely barren of benthic foraminifera. Except for a few Rose Bengal-stained specimens, there were no living benthic species found either in MUC 12 or MC 886 (Melaniuk, 2021) (Table S1). Compared to other Stages, Stage 2 is characterized by relatively high Evenness index (0,78–1,13) and the lowest Shannon index (0,81–1,76). It indicates a homogeneous species composition at Stage 2. Considering that Rose Bengal stains both live and dead cytoplasm, even a few months after the death of the foraminifera, especially in anoxic conditions (Jorissen et al., 1995; Bernhard et al., 2001), it is possible that the few RB-stained individuals were already dead at the time of sampling. There are evidence showing that some of the deep-sea benthic foraminiferal species posses organells such as kleptoplasts, which supports life in oxygen-depleted habitats (LeKieffre et al., 2017). Nevertheless, so far, no additional organelles and/or alternative, anaerobic metabolic pathways has been observed in any of the benthic foraminiferal species from Vestnesa Ridge (Bernhard and Panieri, 2018).

If methane seepage decreases and sulfidic conditions last long enough, they can support the development of chemosynthetic vesicomyid and solemyid clams (Niemann et al., 2006; Treude et al., 2007; Hansen et al., 2017; Hansen et al., 2020), which indicates Stage 3. There is evidence from fossils confirming the presence of chemosynthetic bivalves at Vestnesa Ridge (Ambrose et al., 2015; Hansen et al., 2017; Thomsen et al., 2019; Hansen et al., 2020). Still, clams, have not been observed in modern assemblages from Vestnesa Ridge or other Arctic seep sites (Rybakova et al., 2013; Hansen et al., 2017; Thomsen et al., 2019; Hansen et al., 2020; and references therein). So far, the only obligate chemosynthetic infaunal taxa found at Vestnesa Ridge are the *Siboglinidae* worms and Thyasiridae bivalves that are partially dependent on, or related to chemoautotrophy (Åström et al., 2018). As a result of a progressive decrease in methane flux, oxygen can penetrate the top layer of the sediment. In this study sediments from BC 1088, BC 1098, and BC 1099 correspond to Stage 3 of the environmental successions. The upper 1 to 2-cm layer of the oxygenated sediment provides an environment for a population of benthic foraminifera, and the underlying grey sulfide-rich sediment fuels aggregation of chemosynthetic *Siboglinidae*. As more oxygen is available, the number of foraminifera increased up to 20 individuals per 10 cm^3. Stage 3 is characterized by the highest Shannon index (2,11–2,52) among all Stages of environmental succession and low Evenness index 0,51– 0,65) (Table S1). Similar to Stages 1 and 4, at Stage 3 the dominant species is *C. neoteretis* (13–36%) and *M. barleeanus* (12–51%). Additionally, in sediment from BC 1088 *Bolivina pseudopunctata* constitutes up to 31% of the calcareous species. Species of *Bolivina* sp. are common in areas with dysoxic/anoxic conditions, and are indicators of abundant food supply (Jorissen et al., 2007; Arreguín-Rodríguez and Alegret, 2016). They show ability to perform nitrate respiration (Glock et al., 2019), and thus are considered as indicators of methane-rich environments (Rathburn et al., 2000; Hill et al., 2003; Lobegeier and Sen Gupta, 2008; Wollenburg and Mackensen, 2009).

Stage 4 is represented by sampling sites MUC 8, MUC 10, BC 1081, BC 1082, and showed the typical bright-brown coloring of the top sediment layers, indicating oxygenated sediment from bio-irrigation by the tubeworms, which was

further supported by biogeochemical profiles from the sites (Figures 2A, B) (Melaniuk et al., 2022). Deeper in the core, the sediment color changed to black and grey indicating reducing conditions (Figure 2B). The majority of methane oxidation occurred in the top 4 cm and was decoupled from sulfate reduction, suggesting that MOx was the dominant biological process (Figure 2F, J, S), while the lower parts of the core were subjected to AOM (Melaniuk et al., 2022). Thus, we assume that oxygen was present in the top layers of the core. Rose Bengal-stained foraminifera were present in MUC 8, MUC 10 (A and C), BC 1081, and BC 1082. Similar to Stage 1, the foraminiferal fauna at Stage 4 was dominated by *M. barleeanus* and *C. neoteretis*. *Cassidulina neoteretis* constitutes up to 51% of all foraminifera in MUC 10C, 31% of the foraminifera in MUC 8, 45% in BC 1081, and 32% in BC 1082. Similar to Stage 3, at Stage 4 the Shannon index is high from 1,96 to 2,17, and the Evenness index is low (0,51–0,63) compared to other Stages. Both indices suggest that environmental conditions are very hospitable for foraminifera.

At Stage 4 there were many specimens of the epibenthic species *Cibicides wuellerstorfi* (up to 19% of all calcareous foraminifera in MUC 10A), compared to any other site presented in this study, including the control site with no seepage of methane. *Cibicides wuellerstorfi* is an epifaunal species, which tend to attach itself to structures extending above the seafloor. It prefers low food supply brought by currents and a high oxygen concentration (Lutze and Thiel, 1989; Hald and Steinsund, 1996; Klitgaard-Kristensen et al., 2002; Wollenburg and Mackensen, 2009). Thus, it is not a species expected to be exclusively associated with methane-affected environments. Apparently, the *Siboglinidae* tubeworms aggregations elevated high above the sediment provide a surface for attachment of *C. wuellerstorfi* (Melaniuk et al., 2022).

It was previously suggested that agglutinated foraminifera are less abundant in sediments influenced by methane seepage than calcareous specimens (Dessandier et al., 2019; and references therein). Our study shows the sediment from the *Siboglinidae* field (Stage 3) is more densely populated by agglutinated specimens compared to the samples from sulfur-bacterial mats (MUC 12) (Table S1). In the upper 0–1 cm interval (MUC 8 and MUC 10A, B), living (RB-stained) agglutinated specimens constitute more than 50% of the foraminiferal fauna (Figure 4). The high number of agglutinated specimens may result from the elevated ambient pCO_2 from CO_2 produced during MOx. The elevated pCO_2 could create acidification of the pore water, which can inhibit calcification, eventually causing dissolution of the calcareous species and give agglutinated species a competitive advantage (Figure 4; Table S1). The most abundant species among the agglutinated foraminifera are specimens which belong to the *Reophax* genus. They constitute up to 36% of the total benthic foraminiferal fauna at Stage 3 and up to 37% at the control site (Table S1).

Although our interpretation is based on a limited number of samples similar patterns of environmental successions of seep environments has been found at Ha°Ckon Mosby Mud Volcano (HMMV) located south of Svalbard at 72°N (Wollenburg and Mackensen, 2009). Sites from this area display strict horizontal and vertical distribution patterns according to microhabitat distributions i.e, the hummocky peripheral part with abundant *Siboglinidae* tube worms, a middle sulfidic zone with AOM and sulfur-bacterial mats, and the active center with visible gas bubbles that is sulfate-free and dominated by aerobic methane-oxidizing bacteria (Pimenov et al., 1999; Gebruk et al., 2003; Jerosch et al., 2007).

The middle sulfidic zone of the HMMV corresponds to Stage 2 of the environmental succession, corresponding to cores MUC 12A, B, MC 893B, and MC 886 in this study. In this zone fluid flow is relatively high and sulfate is still present in the sediment and available for AOM (Niemann et al., 2006). Similar to our MUC 12, the middle zone is covered by sulfur-bacterial mats and is practically barren of foraminifera. Only a few individuals of *C. neoteretis* have been found in dysoxic sediments in the upper 1-cm surface layer of this zone (Wollenburg and Mackensen, 2009). Sediments at the peripheral zone of the HMMV with low fluid flow and no AOM activity in the surface sediment (Niemann et al., 2006) corresponds to Stage 4 in our study. Sediment were oxidized down to 10 cm depth and inhabited by *Siboglinidae* tubeworms (Wollenburg and Mackensen, 2009). Similar to Stage 4 (MUC 10 and 8) presented in this paper, Rose Bengal-stained *Fontbotia wuellerstorfi* (i.e, *C. wuellerstorfi*) were abundant and quite a large proportion of the individuals were attached to the *Siboglinidae* tubes.

Stage 5 has not been observed in our study as we have targeted the most active pockmarks at Vestnesa Ridge. To find succession Stage 4, formerly active, but presently inactive pockmarks found at the deeper part of the ridge at 1300 m water depth (Bünz et al., 2012; Consolaro et al., 2015) should be sampled. In the study of Consolaro et al. (2018), the benthic foraminiferal faunas from an inactive pockmark near the core top (and not stained) from this area consists of almost equal proportions of *C. neoteretis*, and *C. reniforme* (each c. 20%) accompanied by lower percentages of *M. barleeanus* (15%) and *C. wuellerstorfi* (10%). Agglutinated specimens constitute only 7% of the fauna.

Ecological succession and its significance in palaeoceanographic interpretation

Based on the results of this work, it becomes apparent that none of these faunal characteristics can be used exclusively as indicators of strength of methane emission. A clear link between strength of methane seepage and distribution of modern benthic foraminifera has not been found to allow the use of fossil

foraminiferal faunas for the reconstruction of past methane emission. It seems that foraminifera are indeed attracted to methane-oxidizing bacteria as a potential food source, as suggested earlier (e.g, Hill et al., 2003; Bernhard et al., 2010), but only when methane seepage is moderate or low as we show for MC 893A of succession Stage 1. Also, during high methane flux and intense AOM activity, oxygen is no longer available for foraminifera in addition to high levels of toxic H_2S within the sediment, and hence the foraminiferal population is radically reduced, or samples are barren of foraminifera.

Furthermore, it was not possible to identify any particular species, or a group of species, that could potentially indicate presence of methane seepage and, there was no endemic species, and the observed species were similar to those from other non-seep locations within the Nordic Seas. The benthic foraminiferal fauna was dominated by species adapted to high organic carbon content and low oxygen conditions, and the key species were *M. barleeanus*, C. *neoteretis*, *Reophax* sp, and in one case *B. pseudopunctata*.

Nevertheless, some subtle differences between seep and non-seep sites do exist, for example at Stage 4 of environmental successions, presence of a chemosynthetic macrofauna such as *Siboglinidae* tubes generating secondary hard substrates arguably support *Cibicides* sp. communities. Increased numbers of *Cibicidoides wuellerstorfi* were observed both at site MUC 8 and 10 as well in previously studies of the Ha° Ckon Mosby Mud Volcano (Wollenburg and Mackensen, 2009). Additionally, compared to other sites samples collected from *Siboglinidae* tubeworm fields (Stage 4 of the environmental successions of seeps) were characterized by a high number of agglutinated foraminifera. This characteristic, however, can probably rarely be used as a methane seepage indicator. Many agglutinated foraminiferal species are often not preserved in fossil records due to their fragile structures (Gooday, 1994), while calcareous species may not preserve due to the elevated ambient pCO_2 (a high ratio of carbon dissolution is common in deep-sea settings including non-seep sites within the Arctic) (Zamelczyk et al., 2013).

Conclusions

Our study shows that the distribution patterns and the species composition of the foraminiferal faunas change according to the progressing environmental succession model of seep environments. Overall, progressing environmental successions result in patchy distributions of living benthic foraminifera; from barren samples in areas with dense sulfur-bacterial mats in sediments affected by AOM and very strong seepage of methane (Stage 2) to high densities in sediment samples from *Siboglinidae* tubeworm fields with MOx as a dominant process and moderate seepage (Stage 4). The main characteristic of each stage of methane seep environments are as follows:

- **At Stage 1** with scattered patches of sulfur-bacterial mats, the species composition of the benthic foraminiferal assemblages is similar to the non-seep locations in the Arctic and Nordic Seas with main dominant species *Cassidulina neoteretis*, and *Melonis barleeanus* being adapted to low oxygen and high organic content. The density of foraminifera is lower compared to other Stages of environmental succession.
- **At Stage 2** with presence of dense sulfur-bacterial mats presence of hydrogen sulfide (H_2S) produced by anaerobic methane oxidation (AOM) is the main limiting factor controlling foraminiferal populations at Vestnesa Ridge with foraminifera-barren or almost barren samples. This Stage is characterized by the lowest Shannon index and highest Evenness index.
- **Stages 3,** with the 1–2 cm top sediment layer oxygenated and the underlying sediment anoxic, the foraminiferal fauna is similar to Stage 1 and Stage 4. The Shannon index is high compared to the control side, but with a low Evenness index.
- **At Stage 4** with moderate methane seepage, and with presence of numerous chemosynthetic *Siboglinidae* tubeworms, a rich foraminiferal community is found. Large numbers of *C. neoteretis*, *M. barleeanus*, and the agglutinated genus *Reophax* sp. were found and in high percentages. The presence of *Siboglinidae* tubes supports the epifaunal benthic foraminiferal species *Cibicides wuellerstorfi* by generating a secondary hard bottom. Similar to Stage 3, the The Shannon index is higher compared to the control side and the Evenness index is low compared to the other Stages.

Foraminifera from the same 1-cm thick interval in a sediment core may represent short-term changes in the foraminiferal population due to the different stages of environmental successions and/or a mix of several different degrees of strengths of methane seepage events. Overall, none of the faunal characteristics can be used exclusively as an indicator of methane emission, strength of methane release, and stages of methane emissions. This makes it difficult to use the foraminiferal fauna compositions as a single tool for reconstructions of past methane release and its intensity.

Data availability statement

The original contributions presented in the study are included in the article/Supplementary Material. Further inquiries can be directed to the corresponding author.

Author contributions

Author contributions to the manuscript was as follows: KM and TLR designed the study. KS, TT, and SS collected and processed samples. KM analyzed data and prepared the manuscript with input from all co-authors. TLR obtained funding for the study. All authors contributed to the article and approved the submitted version.

Funding

Funding of this project was provided by Tromsø Research Foundation (Tromsø Forskningsstiftelse, TFS) to the Paleo-CIRCUS project 2010–2014 and with further support from the Research Council of Norway through its Centers of Excellence funding scheme, grant number 223259 (KM, KS, TLR). Support was also provided through the Cluster of Excellence "The Future Ocean" funded by the German Research Foundation and through the Alexander von Humboldt Foundation (TT, SS).

Acknowledgments

We would like to thank the captain, crew, chief scientist (O. Pfannkuche) and scientific party of the RV *Poseidon* PO419 expedition for technical support and the crew and scientific staff from RV *Helmer Hanssen* in 2015 and 2018 for their help in sampling. M. Veloso, V. Bertics, and K. Kretschmer are thanked for subsampling of sediment. J. Hommer and B. Domeyer are thanked for geochemical analyses. We also acknowledge J. M. Bernhard for hosting and guiding K. Sztybor at WHOI.

Conflict of interest

The authors declare that the research was conducted in the absence of any commercial or financial relationships that could be construed as a potential conflict of interest.

Publisher's note

Supplementary material

The Supplementary Material for this article can be found online at: https://www.frontiersin.org/articles/10.3389/fmars.2022.999902/full#supplementary-material

References

Alve, E., Sergei, K., Schönfeld, J., Dijkstra, N., Golikova, E., Hess, S., et al. (2016). Foram-AMBI: A sensitivity index based on benthic foraminiferal faunas from north-East Atlantic and Arctic fjords, continental shelves and slopes. *Mar. Micropaleontol* 122, 1–12. doi: 10.1016/j.marmicro.2015.11.001

Ambrose, W. G., Panieri, G., Schneider, A., Plaza-Faverola, A., Carroll, M. L., Åström, E. K. L., et al. (2015). Bivalve shell horizons in seafloor pockmarks of the last glacial-interglacial transition: A thousand years of methane emissions in the a rctic O cean. *Geochem Geophys Geosyst* 16 (12), 4108–4129. doi: 10.1002/2015GC005980

Arreguín-Rodríguez, G. J., and Alegret, L. (2016). Deep-sea benthic foraminiferal turnover across early Eocene hyperthermal events at northeast Atlantic DSDP site 550. *Palaeogeogr Palaeoclimatol Palaeoecol.* 451, 62–72. doi: 10.1016/j.palaeo.2016.03.010

Åström, E. K. L., Carroll, M. L., Ambrose, W. G., and Carroll, J. (2016). Arctic Cold seeps in marine methane hydrate environments: Impacts on shelf macrobenthic community structure offshore Svalbard. *Mar. Ecol. Prog. Ser.* 552, 1–18. doi: 10.3354/meps11773

Åström, E. K. L., Carroll, M. L., Ambrose, W. G., Sen, A., Silyakova, A., and Carroll, J. (2018). Methane cold seeps as biological oases in the high-Arctic deep sea. *Limnology Oceanogr* 63 (S1), S209–S231. doi: 10.1002/lno.10732

Bergquist, D. C., Andras, J. P., McNelis, T., Howlett, S., van Horn, M. J., and Fisher, C. R. (2003). Succession in gulf of Mexico cold seep vestimentiferan aggregations: The importance of spatial variability. *Mar. Ecol.* 24 (1), 31–445. doi: 10.1046/j.1439-0485.2003.03800.x

Bernhard, J. M., Buck, K. R., and Barry, J. P. (2001). Monterey Bay cold-seep biota: Assemblages, abundance, and ultrastructure of living foraminifera. *Deep Sea Res. Part I: Oceanographic Res. Papers* 48 (10), 2233–22495. doi: 10.1016/S0967-0637(01)00017-6

Bernhard, J. M., Martin, J. B., and Rathburn, A. E. (2010). Combined carbonate carbon isotopic and cellular ultrastructural studies of individual benthic foraminifera: 2. toward an understanding of apparent disequilibrium in hydrocarbon seeps. *Paleoceanography* 25, PA4206. doi: 10.1029/2010PA001930

Bernhard, J. M., and Panieri, G. (2018). Keystone Arctic paleoceanographic proxy association with putative methanotrophic bacteria. *Sci. Rep.* 8 (1), 10610. doi: 10.1038/s41598-018-28871-3

Bowden, D. A., Rowden, A. A., Thurber, A. R., Baco, A. R., Levin, L. A., Smith, C. R., et al. (2013). Cold seep epifaunal communities on the hikurangi margin, new Zealand: Composition, succession, and vulnerability to human activities. *PloS One* 8 (10), e76869. doi: 10.1371/journal.pone.0076869

Bünz, S., Polyanov, S., Vadakkepuliyambatta, S., Consolaro, C., and Mienert, J. (2012). Active gas venting through hydrate-bearing sediments on the vestnesa ridge, offshore W-Svalbard. *Mar. Geol.* 332–334. doi: 10.1016/j.margeo.2012.09.012

Chapman, M. G., and Underwood, A. J. (1994). Dispersal of the intertidal snail, *Nodilittorina pyramidalis*, in response to the topographic complexity of the substratum. *J. Exp. Mar. Biol. Ecol.* 179 (2), 145–169. doi: 10.1016/0022-0981(94)90111-2

Cline, J. D. (1969). Spectrophotometric determination of hydrogen sulfide in waters. *Limnology Oceanogr* 14 (3), 454–458. doi: 10.4319/lo.1969.14.3.0454

Consolaro, C., Rasmussen, T. L., and Panieri, G. (2018). Palaeoceanographic and environmental changes in the eastern fram strait during the last 14,000years based on benthic and planktonic foraminifera. *Mar. Micropaleontol* 139, 84–101. doi: 10.1016/j.marmicro.2017.11.001

Consolaro, C., Rasmussen, T. L., Panieri, G., Mienert, J., Bünz, S., and Sztybor, K. (2015). Carbon isotope ($\delta^{13}C$) excursions suggest times of major methane release during the last 14 kyr in fram strait, the deep-water gateway to the Arctic. *Clim. Past* 11 (4), 669–685. doi: 10.5194/cp-11-669-2015

Corliss, B. H., Martinson, G., and Keffer, T. (1986). Late quaternary deep-ocean circulation. *GSA Bull.* 97 (9), 1106–11215. doi: 10.1130/0016-7606(1986)97<1106:LQDC>2.0.CO;2

Dayton, P. K., and Hessler, R. R. (1972). Role of biological disturbance in maintaining diversity in the deep sea. *Deep Sea Res. Oceanographic Abstracts*. doi: 10.1016/0011-7471(72)90031-9

Dessandier, P.-A., Borrelli, C., Kalenitchenko, D., and Panieri, G. (2019). Benthic foraminifera in Arctic methane hydrate bearing sediments. *Front. Mar. Sci.* 6, 765. doi: 10.3389/fmars.2019.00765

Dickens, G. R., Castillo, M. M., and Walker, J. C. G. (1997). A blast of gas in the latest Paleocene: Simulating first-order effects of massive dissociation of oceanic methane hydrate. *Geology* 25 (3), 259–2625. doi: 10.1130/0091-7613(1997)025<0259:ABOGIT>2.3.CO;2

Eiken, O., and Hinz, K. (1993). Contourites in the fram strait. *Sedimentary Geol* 82 (1), 15–32. doi: 10.1016/0037-0738(93)90110-Q

Etiope, G. P., Fattorini, D., Regoli, F., Vannoli, P., Italiano, F., Locritani, M., et al. (2014). A thermogenic hydrocarbon seep in shallow Adriatic Sea (Italy): Gas origin, sediment contamination and benthic foraminifera. *Mar. Petroleum Geol* 57, 283–293. doi: 10.1016/j.marpetgeo.2014.06.006

Gebruk, A. V., Krylova, E. M., Lein, A. Y., Vinogradov, G. M., Anderson, E., Pimenov, N. V., et al. (2003). Methane seep community of the håkkon mosby mud volcano (the Norwegian sea): composition and trophic aspects. *Sarsia* 88, 394–403. doi: 10.1080/00364820310003190

Glock, N., Roy, A. S., Romero, D., Wein, T., Weissenbach, J., Revsbech, N. P., et al. (2019). Metabolic preference of nitrate over oxygen as an electron acceptor in foraminifera from the Peruvian oxygen minimum zone. *Proc. Natl. Acad. Sci. U.S.A.* 116, 2860–2865. doi: 10.1073/pnas.1813887116

Gooday, A. J. (1994). The biology of deep-Sea foraminifera: A review of some advances and their applications in paleoceanography. *PALAIOS* 9 (1), 14–31. doi: 10.2307/3515075

Gooday, A. J., and Jorissen, F. J. (2012). Benthic foraminiferal biogeography: Controls on global distribution patterns in deep-water settings. *Annu. Rev. Mar. Sci.* 4 (1), 237–2625. doi: 10.1146/annurev-marine-120709-142737

Hald, M., and Steinsund, P. I. (1996). Benthic foraminifera and carbonate dissolution in the surface sediments of the barents and kara seas. *Berichte zur Polarforschung* 212, 285–307.

Hansen, J., Hoff, U., Sztybor, K., and Rasmussen, T. L. (2017). Taxonomy and palaeoecology of two late pleistocene species of vesicomyid bivalves from cold methane seeps at Svalbard (79 n). *J. Molluscan Stud.* 83 (3), 270–2795. doi: 10.1093/mollus/eyx014

Hansen, J., Mohamed, M. E., Åström, E. K. L., and Rasmussen, T. L. (2020). New late pleistocene species of acharax from Arctic methane seeps off Svalbard. *J. Systematic Palaeontol* 18 (2), 197–2125. doi: 10.1080/14772019.2019.1594420

Herguera, J. C., Paull, C., Perez, E., Ussler, I. I. I. W., and Peltzer, E. T. (2014). Limits to the sensitivity of living benthic foraminifera to pore water carbon isotope anomalies in methane vent environments. *Paleoceanography* 29 (3), 273–2895. doi: 10.1002/2013PA002457

Hill, T. M., Kennett, J. P., and Spero, H. J. (2003). Foraminifera as indicators of methane-rich environments: A study of modern methane seeps in Santa Barbara channel, California. *Mar. Micropaleontol* 49 (1), 123–1385. doi: 10.1016/S0377-8398(03)00032-X

Hustoft, S., Bünz, S., Mienert, J., and Chand, S. (2009). Gas hydrate reservoir and active methane-venting province in sediments on <20 ma young oceanic crust in the fram strait, offshore NW-Svalbard. *Earth Planetary Sci. Lett.* 284 (1), 12–24. doi: 10.1016/j.epsl.2009.03.038

Jørgensen, B. B. (1978). A comparison of methods for the quantification of bacterial sulfate reduction in coastal marine sediments. *Geomicrobiol J.* 1, 11–27. doi: 10.1080/01490457809377721

Jakobsson, M., Mayer, L. A., Bringensparr, C., Castro, C. F., Mohammad, R., Johson, P., et al. (2020). The international bathymetric chart of the Arctic ocean version 4.0. *Sci. Data* 7 (1), 176. doi: 10.1038/s41597-020-0520-9

Jerosch, K., Schlüter, M., Foucher, J.-P., Allais, A.-G., Klages, M., and Edy, C. (2007). Spatial distribution of mud flows, chemoautotrophic communities, and biogeochemical habitats at Håkon Mosby Mud Volcano. *Marine Geology* 243 (1–4), 1–17. doi: 10.1016/j.margeo.2007.03.010

Jorissen, F. J., de Stigter, H. C., and Widmark, J. G. V. (1995). A conceptual model explaining benthic foraminiferal microhabitats. *Mar. Micropaleontol* 26 (1), 3–155. doi: 10.1016/0377-8398(95)00047-X

Jorissen, F. J., Fontanier, C., and Thomas, E. (2007). "Paleoceanographical proxies based on deep- sea benthic foraminiferal assemblages characteristics," in *Proxies in late Cenozoic paleoceanography: Part 2: Biological tracers and biomarkers*. Eds. C. Hillaire-Marcel and A. Vernal (Amsterdam, Netherlands: Elsevier), 263–326.

Kallmeyer, J., Ferdelman, T. G., Weber, A., Fossing, H., and Jørgensen, B. B. (2004). A cold chromium distillation procedure for radiolabeled sulfide applied to sulfate reduction measurements. *Limnology Oceanogr: Methods* 2 (6), 171–1805. doi: 10.4319/lom.2004.2.171

Klitgaard-Kristensen, D., Sejrup, H. F., and Haflidason, H. (2002). Distribution of recent calcareous benthic foraminifera in the northern north Sea and relation to the environment. *Polar Res.* 21, 275–282. doi: 10.1111/j.1751-8369.2002.tb00081.x

LeKieffre, C., Spangenberg, J. E., Mabilleau, G., Escrig, S., Meibom, A., and Geslin, E. (2017). Surviving anoxia in marine sediments: The metabolic response of ubiquitous benthic foraminifera (*Ammonia tepida*). *PloS One* 12 (5), e0177604. doi: 10.1371/journal.pone.0177604

Levin, L. A. (2005). "Ecology of cold seep sediments: Interactions of fauna with flow, chemistry and microbes," in *Oceanography and marine biology: An annual review*. Eds. R. N. Gibson, R. J. A. Atkinson and J. D. M. Gordon (Boca Raton: CRC Press-Taylor & Francis Group), 1–46. doi: 10.1201/9781420037449.ch1

Lobegeier, M. K., and Sen Gupta, B. K. (2008). Foraminifera of hydrocarbon seeps, gulf of Mexico. *J. Foraminiferal Res.* 38 (2), 93–116. doi: 10.2113/gsjfr.38.2.93

Lutze, G. F., and Thiel, H. (1989). Epibenthic foraminifera from elevated microhabitats; cibicidoides wuellerstorfi and *Planulina ariminensis*. *J. Foraminiferal Res.* 19 (2), 153–1585. doi: 10.2113/gsjfr.19.2.153

Mackensen, A., Sejrup, H. P., and Jansen, E. (1985). The distribution of living benthic foraminifera on the continental slope and rise off southwest Norway. *Mar. Micropaleontol* 9 (4), 275–3065. doi: 10.1016/0377-8398(85)90001-5

Martin, R. A., Nesbitt, E. A., and Campbell, K. A. (2010). The effects of anaerobic methane oxidation on benthic foraminiferal assemblages and stable isotopes on the hikurangi margin of eastern new Zealand. *Mar. Geol* 272 (1), 270–2845. doi: 10.1016/j.margeo.2009.03.024

Melaniuk, K. (2021). Effectiveness of fluorescent viability assays in studies of Arctic cold seep foraminifera. *Front. Mar. Sci.* 8 (198). doi: 10.3389/fmars.2021.587748

Melaniuk, K., Sztybor, K., Treude, T., Sommer, S., and Rasmussen, T. L. (2022). Influence of methane seepage on isotopic signatures in living deep-sea benthic foraminifera, 79° n. *Sci. Rep.* 12, 1169. doi: 10.1038/s41598-022-05175-1

Millo, C., Sarnthein, M., Erlenkeuser, H., Grootes, P. M., and Andersen, N. (2005). Methane-induced early diagenesis of foraminiferal tests in the southwestern Greenland Sea. *Mar. Micropaleontol* 58 (1), 1–12. doi: 10.1016/j.marmicro.2005.07.003

Murray, J. W. (2006). *Ecology and applications of benthic foraminifera* (Cambridge: Cambridge University Press).

Niemann, H., Lösekann, T., de Beer, D., Elvert, M., Nadalig, T., Knittel, K., et al. (2006). Novel microbial communities of the haakon mosby mud volcano and their role as a methane sink. *Nature* 443 (7113), 854–8585. doi: 10.1038/nature05227

Pimenov, N., Savvichev, A., Rusanov, I., Lein, A., Egorov, A., Gebruk, A., et al. (1999). Microbial processes of carbon cycle as the base of food chain of håkon mosby mud volcano benthic community. *Geo-Mar Lett.* 19, 89–96. doi: 10.1007/s003670050097

Plaza-Faverola,A., Bünz, S., Johnson, J. E., Chand, S., Knies, J., Mienert, J., and Franek, P. (2015). Role of tectonic stress in seepage evolution along the gas hydrate-charged vestnesa ridge, fram strait. *Geophys Res. Lett.* 42 (3), 733–7425. doi: 10.1002/2014GL062474

Rasmussen, T. L., and Thomsen, E. (2017). Ecology of deep-sea benthic foraminifera in the north Atlantic during the last glaciation: Food or temperature control. *Palaeogeogr Palaeoclimatol Palaeoecol.* 472, 15–32. doi: 10.1016/j.palaeo.2017.02.012

Rathburn, A. E., Levin, L. A., Held, Z., and Lohmann, K. C. (2000). Benthic foraminifera associated with cold methane seeps on the northern California margin: Ecology and stable isotopic composition. *Mar. Micropaleontol* 38 (3), 247–2665. doi: 10.1016/S0377-8398(00)00005-0

Rybakova, E., Galkin, S., Bergmann, M., Soltwedel, T., and Gebruk, A. (2013). Density and distribution of megafauna at the håkon mosby mud volcano (the barents Sea) based on image analysis. *Biogeosciences* 10, 3359–3374. doi: 10.5194/bg-10-3359-2013

Schneider, A., Crémière, A., Panieri, G., Lepland, A., and Knies, J. (2017). Diagenetic alteration of benthic foraminifera from a methane seep site on vestnesa ridge (NW Svalbard). *Deep Sea Res. Part I: Oceanographic Res. Papers* 123, 22–34. doi: 10.1016/j.dsr.2017.03.001

Schönfeld, J., Alve, E., Geslin, E., Jorissen, F., Korsu, S., Spezzaferri, S., et al. (2012). The FOBIMO (FOraminiferal BIo-MOnitoring) initiative–towards a standardised protocol for soft-bottom benthic foraminiferal monitoring studies. *Mar. Micropaleontol* 94–95, 1–13. doi: 10.1016/j.marmicro.2012.06.001

Smith, L. M., Sachs, J. P., Jennings, A. E., Anderson, D. M., and deVernal, A. (2001). Light $\delta^{13}C$ events during deglaciation of the East Greenland continental shelf attributed to methane release from gas hydrates. *Geophys Res. Lett.* 28 (11), 2217–2220. doi: 10.1029/2000GL012627

Somero, G. N., Childress, J. J., and Anderson, A. E. (1989). Transport, metabolism, and detoxification of hydrogen sulfide in animals from sulfide-rich marine environments. *Rev. Aquat. Sci. RAQSEL* 1 (4).

Sommer, S., Linke, P., Pfannkuche, O., Schleicher, T., Schneider, J., Deimling, V., et al. (2009). Seabed methane emissions and the habitat of frenulate tubeworms on the captain arutyunov mud volcano (Gulf of cadiz). *Mar. Ecol. Prog. Ser.* 382, 69–86. doi: 10.3354/meps07956

Sztybor, K., and Rasmussen, T. L. (2017). Diagenetic disturbances of marine sedimentary records from methane-influenced environments in the fram strait as indications of variation in seep intensity during the last 35 000 years. *Boreas* 46 (2), 212–2285. doi: 10.1111/bor.12202

Tanner, J. E., Hughes, T. H., and Connell, J. H. (1994). Species coexistence, keystone species, and succession: A sensitivity analysis. *Ecology* 75 (8), 2204–22195. doi: 10.2307/1940877

Thomas, E., Booth, L., Maslin, M., and Shackleton, N. J. (1995). Northeastern Atlantic benthic foraminifera during the last 45,000 years: Changes in productivity seen from the bottom up. *Paleoceanography* 10 (3), 545–5625. doi: 10.1029/94PA03056

Thomsen, E., Rasmussen, T. L., Sztybor, K., Hanken, N.-M., Tendal, O. S., and Uchman, A. (2019). Cold-seep fossil macrofaunal assemblages from vestnesa ridge, eastern fram strait, during the past 45 000 years. *Polar Res.* 38 (0). doi: 10.33265/polar.v38.3310

Torres, M. E., Mix, A. C., Kinports, K., Haley, B., Klinkhammer, G. P., McManus, J., et al. (2003). Is methane venting at the seafloor recorded by δ13C of benthic foraminifera shells? *Paleoceanography* 18 (3). doi: 10.1029/2002PA000824

Treude, T., Krause, S., Steinle, L., Burwicz, E., Hamdan, L. J., Niemann, H., et al. (2020). Biogeochemical consequences of nonvertical methane transport in sediment offshore northwestern Svalbard. *J. Geophys Research: Biogeosci* 125 (3), e2019JG005371. doi: 10.1029/2019JG005371

Treude, T., Orphan, V., Knittel, K., Gieseke, A., House, C. H., and Boetius, A. (2007). Consumption of methane and CO_2 by methanotrophic microbial mats from gas seeps of the anoxic black Sea. *Appl. Environ. Microbiol.* 73 (7), 2271–2283. doi: 10.1128/AEM.02685-06

Wefer, G., Heinze, P.-M., and Berger, W. H. (1994). Clues to ancient methane release. *Nature* 369 (6478), 282–282. doi: 10.1038/369282a0

Wollenburg, J. E., and Mackensen, A. (1998). Living benthic foraminifers from the central Arctic ocean: Faunal composition, standing stock and diversity. *Mar. Micropaleontol* 34 (3), 153–185. doi: 10.1016/S0377-8398(98)00007-3

Wollenburg, J. E., and Mackensen, A. (2009). The ecology and distribution of benthic foraminifera at the håkon mosby mud volcano (SW barents Sea slope). *Deep Sea Res. Part I: Oceanographic Res. Papers* 56 (8), 1336–1370. doi: 10.1016/j.dsr.2009.02.004

Yao, H., Hong, W.-L., Panieri, G., Sauer, S., Torres, M. E., Lehmann, M. F., et al. (2019). Fracture-controlled fluid transport supports microbial methane-oxidizing communities at vestnesa ridge. *Biogeosciences* 16 (10), 2221–2232. doi: 10.5194/bg-16-2221-2019

Zamelczyk, K., Rasmussen, T. L., Husum, K., and Hald, M. (2013). Marine calcium carbonate preservation vs. climate change over the last two millennia in the fram strait: Implications for planktic foraminiferal paleostudies. *Mar. Micropaleontol* 98, 14–27. doi: 10.1016/j.marmicro.2012.10.001